OPEN

Substrate composition directs slime molds behavior

Fernando Patino-Ramirez [ID][1]*, Aurèle Boussard [ID][2], Chloé Arson[1,3] & Audrey Dussutour[2,3]*

Cells, including unicellulars, are highly sensitive to external constraints from their environment. Amoeboid cells change their cell shape during locomotion and in response to external stimuli. Physarum polycephalum is a large multinucleated amoeboid cell that extends and develops pseudopods. In this paper, changes in cell behavior and shape were measured during the exploration of homogenous and non-homogenous environments that presented neutral, and nutritive and/or adverse substances. In the first place, we developed a fully automated image analysis method to measure quantitatively changes in both migration and shape. Then we measured various metrics that describe the area covered, the exploration dynamics, the migration rate and the slime mold shape. Our results show that: (1) Not only the nature, but also the spatial distribution of chemical substances affect the exploration behavior of slime molds; (2) Nutritive and adverse substances both slow down the exploration and prevent the formation of pseudopods; and (3) Slime mold placed in an adverse environment preferentially occupies previously explored areas rather than unexplored areas using mucus secretion as a buffer. Our results also show that slime molds migrate at a rate governed by the substrate up until they get within a critical distance to chemical substances.

Large-scale spatial patterns in biology are common and knowing how these patterns evolve and what are their functional role, enables us to understand the evolution of biocomplexity (see e.g.[1–4]). Morphogenesis has been studied in length at the cell level (see e.g.[5–8]); cells are highly sensitive to geometrical and mechanical constraints from their microenvironment and respond to these conditions by changing shape (see e.g.[9,10]); these transformations impact cell migration and growth (see e.g.[7,11–13]). Cellular migration is a fundamental property of every cell and it is crucial for the development and morphogenesis of animal body plans and organ systems (see e.g.[14–16]). Cell migration is either in a random direction or directed towards localized cues[17–20]. Mechanisms of cellular movement have been mostly studied in chemotactic cells, such as neutrophils[17], bacteria[21], Ciliata[22], fungi[23] and cellular slime molds[19].

Due to its extremely fast migration rate and highly irregular shape, the acellular slime mold *Physarum Polycephalum* represents a prime example of differentiated growth and thus offers an attractive model for the analysis of morphogenesis dynamics underlying cellular migration and exploration[24–28]. *P polycephalum* is a giant single-celled organism that can grow to cover several square meters. Its morphology includes search fronts that are connected to a system of intersecting veins, in which oscillatory flows of the protoplasm "shuttle streaming" take place. This vein network allows (1) an efficient distribution of chemical signals, oxygen, nutrients over large distances and (2) cell migration at a speed of few centimeters per hour[29,30]. The driving force for this protoplasm streaming is a periodic, peristaltic contraction and relaxation of the veins due to the actin-myosin interaction, which is regulated by oscillations of intracellular chemicals such as calcium[31–33]. As it explores its environment, the slime mold extends temporary arm-like projections named pseudopods. It also secretes continuously a thick extracellular slime[34]. The glycoprotein nature of the extracellular slime coat endows *P polycephalum* with unique protective and structural properties that favor survival of the migrating, naked slime mold[35]. As the slime mold is foraging, it avoids areas covered with this mucus, which marks previously explored areas[36,37].

In the presence of chemical substances in the environment, *P. Polycephalum* shows directional movements towards or away from the stimuli (i.e. chemotaxis). *Physarum* morphology, evolution and behaviors are strongly affected by the availability, location and concentration of nutrients. When the slime mold senses attractants (e.g. food cues) using specific receptors located on the membrane, the oscillation frequency in the pseudopod closest to the attractant increases, causing cytoplasm to flow towards the attractant[38]. On the contrary, when repellents

[1]School of Civil and Environmental Engineering, Georgia Institute of Technology, Atlanta, GA, USA. [2]Research Centre on Animal Cognition (CRCA), Centre for Integrative Biology (CBI), Toulouse University, CNRS, UPS, Toulouse, France. [3]These authors contributed equally: Chloé Arson and Audrey Dussutour. *email: fp@gatech.edu; audrey.dussutour@univ-tlse3.fr
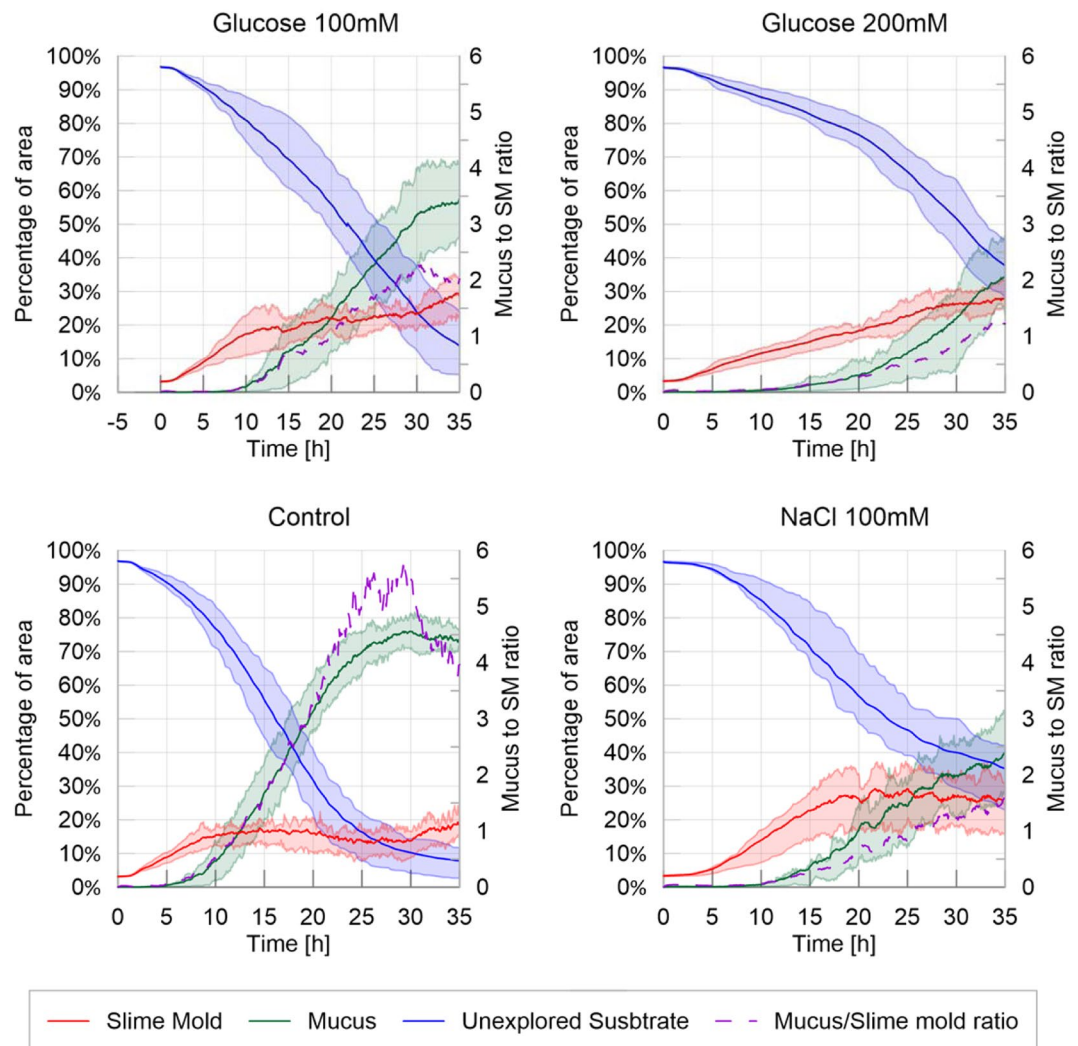
Figure 1. Fraction of area covered by slime mold, mucus and unexplored substrate – Homogeneous environment. The solid lines correspond to the average index calculated over the 20 replicates, while the shaded areas correspond to the first and third quartiles of the data, the dashed line correspond to the ratio between the average mucus area over the average slime mold area over time.

such as salts are sensed, the oscillation frequency decreases and the slime mold moves away from the repellent[38]. Although slime molds lack the complex hardware of animals with brains, they live in environments that are as complex and they face the same decision-making challenges[39]. Hence, acellular slime molds have been the subject of a wide range of studies showing that they can solve complex biological and computational problems without any specialized nervous tissue[24,36,37,40–46].

In this paper the objectives are to characterize the morphology and dynamics of *Physarum* exploring various environments. First, we investigate how movement is affected by homogeneous environmental conditions: adverse environment (using salt as a repellent[47]; nutritive environments (using glucose as a chemo-attractant[48,49] with 2 different concentrations) and a neutral environment (using plain agar). Second, we analyze the geometrical evolution of slime molds placed at a distance from a nutritive spot (glucose), with and without a repelling spot (salt) in between. We characterize slime molds' movement both temporally and spatially, to capture the full dynamics. To this aim, we develop a program that automatically analyzes sequences of images to track the areas covered and explored by the slime mold, the slime mold shape, the refinement and secondary growth cycles, as well as the distance to the nutritive spot.

Results

Homogeneous environment.   In order to study the influence of the environment on slime mold expansion rate, we analyzed the areas covered by slime mold, unexplored substrate and mucus over time, as shown in Fig. 1.

In a neutral (control) and slightly nutritive environment (glucose at 100 mM), the slime molds started to spread from the very beginning of the experiment (Fig. 1; Table 1 and Fig. 5 in S1 Appendix, P > 0.05). By contrast, in a highly nutritive environment (200 mM glucose), slime molds started to explore later (P < 0.001 when
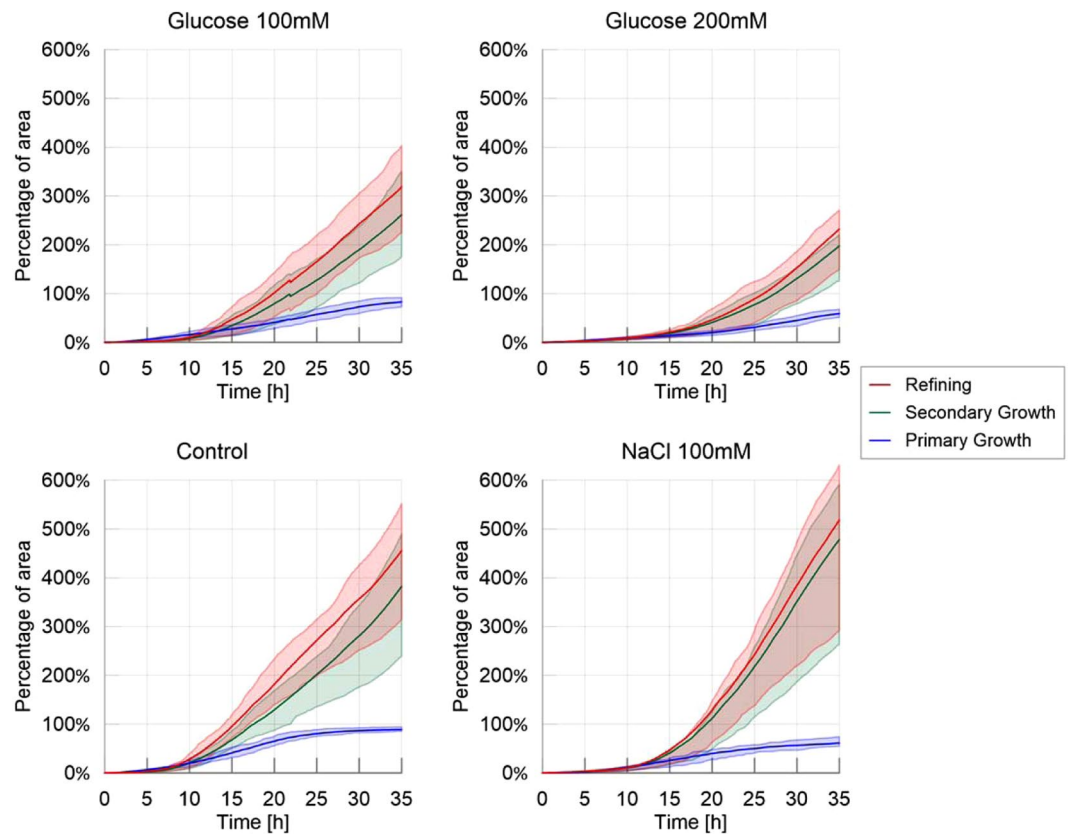
Figure 2. Cumulative areas covered by primary growth, refinement and secondary growth – Homogeneous experiments. The solid line corresponds to the average index calculated over the 20 replicates, while the shaded areas correspond to the first and third quartiles of the data.

compared to the control). Slime molds placed in an adverse environment (100 mM NaCl) were lagging the most and only started exploring after 3 hours ($P < 0.001$ when compared to the control). Once the slime molds started to explore, they all grew at the same rate (Fig. 1; Table 2, Fig. 6 in S1 Appendix, $P > 0.05$ when compared to the control) except the ones placed in a highly nutritive environment which were slowed down ($P < 0.001$ when compared to the control).

At the end of the experiment (after 35 hours), the slime molds reached a similar surface area in a control environment and in an adverse environment (Table 3 and Fig. 7 in S1 Appendix, $P > 0.05$ when compared to the control). Interestingly, after reaching a plateau at 18 hours, the area covered by the slime molds in an adverse environment oscillated with seemingly cyclic fluctuations (Fig. 1). In both a slightly and a highly nutritive environment, the slime molds reached a higher final surface area than the slime molds placed in a control environment ($P < 0.001$ in both comparisons) and covered approximately 30% of arena at the end experiment. It is worth noting that in a highly nutritive environment, the area of the surface covered by the slime molds never reached a plateau after 35 hours, suggesting that the slime molds did not reach its maximum surface area (Fig. 1).

Refinement *i.e.* appearance of mucus, was observed after 5 hours in the control environment. In all other environments, mucus appeared later (Table 4 and Fig. 8 in S1 Appendix: $P < 0.001$ for all treatments when compared to the control). In a highly nutritive environment, mucus was only observed after 10 hours, which marked the strongest delay in the refinement process. Once the mucus started to be apparent, its surface area grew quicker in the control environment than in the other three treatments (Table 5 and Fig. 9 in S1 Appendix; $P < 0.001$ for all treatments when compared to the control). Thus the area of the surface covered by mucus at the end of the experiment was the largest in the control environment where it reached 75% of the arena against 55%, 40% and 35% for the slightly nutritive, the adverse and the highly nutritive environments respectively (Table 6 and Fig. 10 in S1 Appendix; $P < 0.001$ for all treatments when compared to the control).

Hence, slime molds placed in a control environment explored almost all the arena leaving only 5% of the arena unexplored while in the other treatments the area of the surface unexplored were significant: 15%, 35% and 38% for the slightly nutritive, the highly nutritive and the adverse environments respectively. Interestingly, although the growth rate dynamics differed between highly nutritive and adverse environments, the final unexplored surface areas were similar. In a highly nutritive environment the slime molds grew slowly and steadily while in an adverse environment slime molds grew rather quickly but after a long delay.

Next, we analyzed the evolution of the cumulative areas covered by primary growth, refinement and secondary growth (Fig. 2). The cumulative area covered by secondary growth, which reveals the cyclic nature of the exploration process, was the highest in the adverse environment (480% coverage) followed by the control
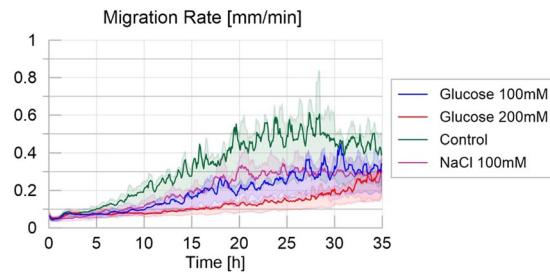
Figure 3. Migration rate over time for the four different treatments, defined as the maximum distance between the contours of the slime mold between two consecutive images divided by their time interval (5 minutes apart), measured in millimeters per minute. The solid line corresponds to the average calculated over 20 replicates per treatment, while the shaded areas correspond to the first and third quartiles of the data.

environment (380%), the slightly nutritive environment (250%) and the highly nutritive environment (180%). All comparisons lead to significant differences $P < 0.05$, except control vs. adverse environment (Table 7 and Fig. 11 in S1 Appendix). This observation confirms that exploration was slowed down by the presence of nutrients, and that the pulsatile behavior (*i.e* the exploration of previously explored area) was stimulated by repellents.

In accordance with the previous results, Fig. 3 (average migration rate for the treatments) shows a higher migration rate for the control treatment than for the other treatments (Table 8 and Fig. 12 in S1 Appendix: $P < 0.001$ for each pairwise comparison). While slime molds exploring the highly nutritive environment were slower than slime molds exploring the slightly nutritive or the adverse environment ($P < 0.001$ each), these two showed no significant differences ($P > 0.05$).

The slime molds exploring the adverse environment showed the highest probability to explore a previously explored substrate than the other treatments as shown in Fig. 4 and Supplementary Materials (Tendency for secondary growth: Table 9 and Fig. 13 in S1 Appendix: $P < 0.001$ for each pairwise comparison). When exploring a highly nutritive environment, slime molds also displayed a significant positive tendency for secondary growth ($P < 0.001$ for each pairwise comparison) but significantly less strong than on the adverse environment ($P < 0.001$). For the other treatments, the measured proportion of secondary growth was not different from the expected proportion of secondary growth, indicating that slime molds did not avoid previously explored substrate and explored randomly (Fig. 13 in S1 Appendix). The peaks observed within the first 5 hours of the experiment correspond to an isotropic extension immediately followed by a refinement process that occurred before the slime mold started to explore continuously its environment. This behavior is often observed when a slime mold is introduced in a new environment and is referred as "contemplative[50]" *i.e.* the slime mold migrates, retracts and moves again. The peak was larger in an adverse environment.

We then analyzed the evolution of the shape of the slime molds contour. Note that the experimental set ups in which slime molds were placed exhibited radial symmetry. Hence, no preferential expansion direction was expected. We thus focused on contour shape, not orientation.

As expected, circularity was initially one in all tests (circular slime mold spot), and increased over time as the contour shape departed from a circle (Fig. 2 in S1 Appendix). In the control and nutritive environments, circularity remained between 1.05 and 1.10, whereas it fluctuated between 1.05 and 1.30 in the adverse environment. This observation suggests that, in an adverse environment, slime molds explored the petri dish by spreading and thinning over larger areas than in the other environments, which led to shape changes and a decrease of slime mold circularity. However fluctuations among the 20 replicates were too high to identify any trend in the evolution of slime mold circularity.

The eccentricity index was initially close to zero (circular cell) and increased up to almost 0.8 over time, with important fluctuations in all the treatments (Fig. 3 in S1 Appendix). Eccentricity is an indicator of the number of pseudopodia. But a non-eccentric convex hull can enclose non-circular contours of slime mold, since pseudopodia can develop in a symmetric fashion. That is why no major difference was noted between the treatments. This result highlights the absence of preferred expansion direction in symmetric, homogeneous environments.

Solidity decreased with the emergence of pseudopodia, since slime mold branching disrupted the initially convex shape of the slime mold (Fig. 5). In the control environment, in which the exploration rate was the highest, the decrease of solidity of the slime mold area was the highest (and the fastest) decreasing from 1 to 0.3 and then becoming relatively stable, with fluctuations of $+/-0.05$ (Table 10 and Fig. 14 in S1 Appendix; $P < 0.01$ for all paired comparisons except adverse environment vs. slightly nutritive environment, where $P > 0.05$). Slower exploration resulted in a slower and steadier loss of solidity as observed in the nutritive and adverse environments. The highly nutritive environment yielded the highest solidity at the end of the experiment (0.6), which confirmed that the presence of glucose slowed down exploration.

We next focused on the number of clusters, corresponding to the number of pseudopodia (Fig. 6). Initially the slime molds stretched as a single cluster. Once mucus started to be apparent, slime molds usually divided up into several clusters, and started the active exploration phase. In highly nutritive and adverse environments, the number of clusters over time was lower than in the other two treatments (new pseudopod number: Table 11 and Fig. 15 in S1 Appendix, and $P < 0.01$ for all paired comparisons except for adverse environment vs. highly nutritive environment). This observation confirmed that the presence of concentrated nutrients slowed down the
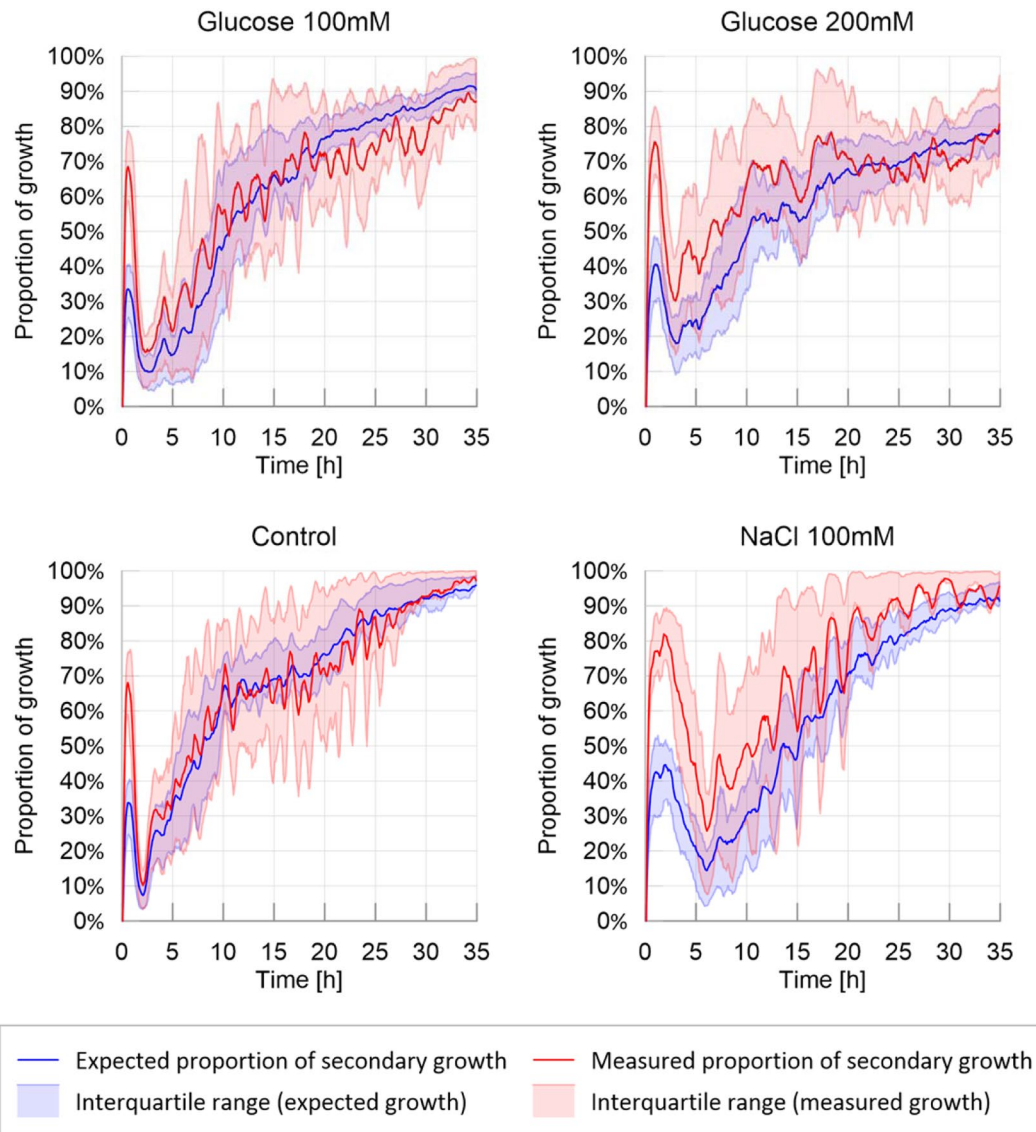
Figure 4. Ratio of secondary growth: observed and expected proportion of secondary growth. The solid line corresponds to the average calculated over 20 replicates per treatment, while the shaded areas correspond to the first and third quartiles of the data.
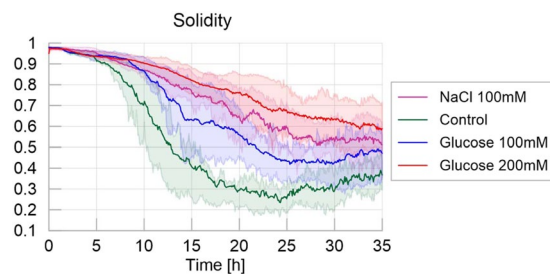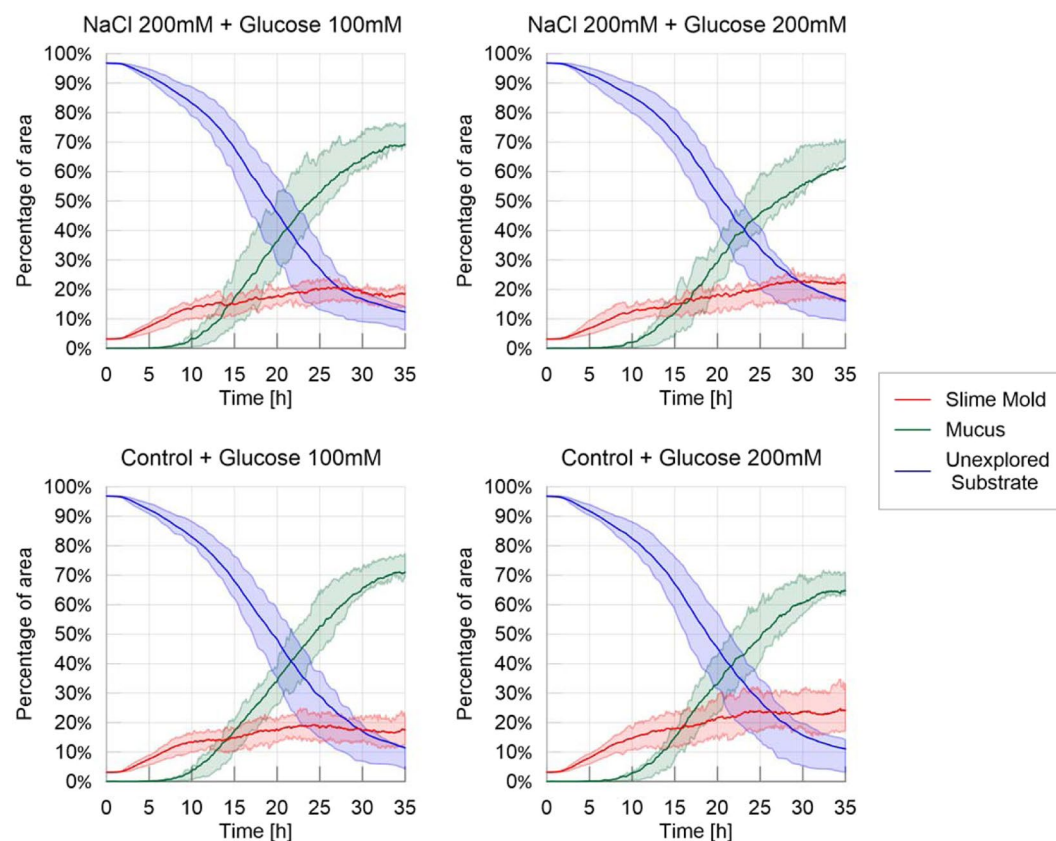

Figure 5. Solidity - Homogeneous experiments. The solid line corresponds to the average index calculated over the 20 replicates, while the shaded areas correspond to the first and third quartiles of the data.

exploration, and that the presence of repellents triggered a highly pulsatile behavior with small exploration fronts, which were sometimes not detected as separate clusters.
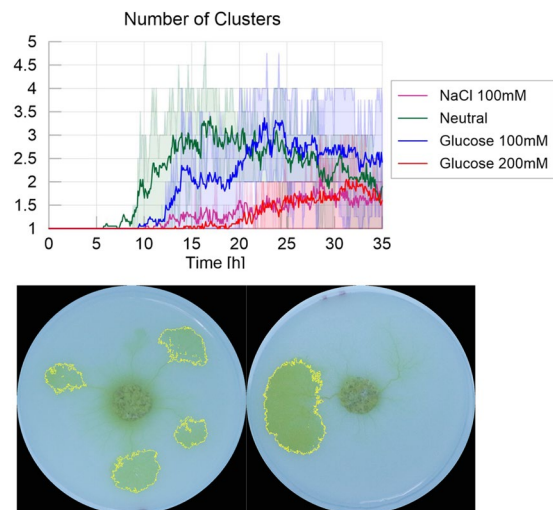
Figure 6. Number of clusters - Homogeneous experiments. The solid line corresponds to the average index calculated over the 20 replicates, while the shaded areas correspond to the first and third quartiles of the data. Pictures show examples of clusters for the Control environment (left) and 200 mM Glucose environment (right).

Figure 7. Fraction of area covered by each entity (slime mold, mucus, unexplored substrate) – Spot experiments. The solid line corresponds to the average index calculated over the 20 replicates, while the shaded areas correspond to the first and third quartiles of the data.

Spot experiments. In the spot experiments, we studied the influence of discrete distributions of nutrients and repellents on exploration dynamics. When looking at the evolution of slime mold, mucus and unexplored substrate over time (Fig. 7), we only observed marginal difference among the treatments, which all exhibited similar patterns of exploration, e.g. similar percentage of non-explored area and similar mucus accumulation. The presence of an adverse spot only delayed the appearance of the first pseudopod (first movement: Table 12 and Fig. 15 in S1 Appendix, $P < 0.05$) but not the first appearance of mucus (first appearance of mucus: Table 15
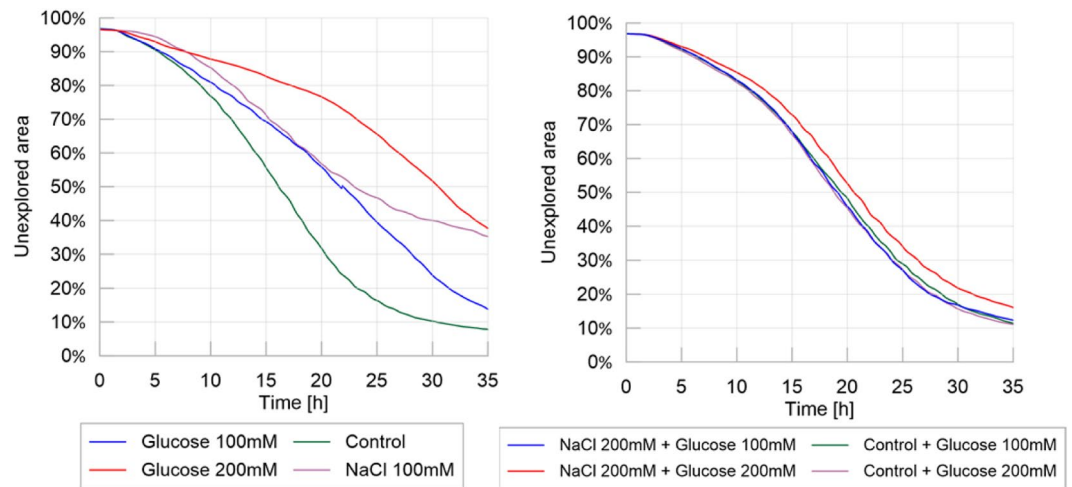
Figure 8. Exploration behavior: homogeneous experiments (left) vs. spot experiments (right). Percentage of unexplored area over time. Mean values of over 20 replicates for each different treatment.

in S1 Appendix, not significant). The only noticeable differences lie in the surface area reached at the end of the experiment: slime molds that were offered a highly nutritive spot grew larger (final surface area: Table 14 and Fig. 17 in S1 Appendix; $P < 0.01$). By contrast, the area of the surface covered by mucus was lower (mucus final surface: Table 17 and Fig. 18 in S1 Appendix; $P < 0.01$) than slime molds that were offered a slightly nutritive spot. In comparison with the experiments conducted in homogeneous environments, we did not observe any expansion/refinement cycles in the spot experiments, meaning that slime mold spread steadily towards the food source despite the presence of an obstacle on the way.

The exploration behavior in the spot experiments was similar to that observed in the control environment in homogeneous experiments as observed in Fig. 8, which includes the average percentage of unexplored area for the homogeneous and spot experiments shown in Figs 1 and 7 respectively. This suggests that the spatial exploration of slime mold depended mostly on the substrate and not on the geometric distribution of the nutritive and adverse stimuli.

The cumulative areas covered by secondary growth for the spot experiments (Fig. 9) were also similar for all treatments (Table 18 in S1 Appendix, $P > 0.05$), suggesting again, that isolated spots with nutritive or adverse stimuli did not alter the overall exploration of slime molds when growing on the same, control, substrate.

The trends of migration rate, as shown in Fig. 10, show that slime molds were not affected by the difference between treatments, showing only a slight effect of the concentration of the food spot ($P < 0.05$), as shown on Table 19 in S1 Appendix. This effect showed that the migration rate was slightly superior when slime molds were offered a higher than a lower nutritive spot.

Similarly, looking at the predilection of slime molds to grow towards mucus (secondary growth), as shown in Fig. 11, no significant differences were observed between treatments (Table 19 in S1 Appendix), which suggests that the growth type is not influenced by the existence or concentration of discrete attracting/repelling spots.

The results obtained for the four different shape indexes (Fig. 4 in S1 Appendix) for the spot experiments support the hypothesis that discrete spots of nutrients or repellents did not affect the overall expansion dynamics and exploration cycles. This interpretation is confirmed by the average number of pseudopods, which was found to be correlated to the formation of mucus during the exploration phase: in all the spot experiments, the number of clusters increases from 1 to 2.5 within around 12 hours, to reach a plateau afterwards. In other words, less exploration cycles were observed in non-homogenous environments, yielding less pseudopodia.

The evolution of the shortest distance from the slime mold cell to the glucose spot is shown in Fig. 12, which can be viewed as a "survival" plot, displaying the proportion of the replicate (P) in which slime mold has not reached the nutritive spot at a given time. Both increasing the concentration of nutrient in the spot (from slightly nutritive to highly nutritive) and adding an aversive spot increased the time to reach the food patch by decreasing the probability to reach it (time to food patch: Table 22 and Fig. 18 in S1 Appendix, nutritive: $P < 0.01$; aversive: $P < 0.05$).

Discussion

Exploration in slime molds involves two different processes: area extension and movement[27]. Slime molds locomotion and morphogenesis depend on the response of the organism to the environmental conditions such as light, hygrometry, pH, or the presence of chemicals[29,51]. In the present paper, we show that distributions of nutritive and aversive cues affected drastically the exploration pattern of slime molds.

The typical exploration behavior of a slime mold (in control conditions) started by a stretching period where the slime molds grew uniformly in all directions for 10 hours. Then, the contour of slime mold lost circularity when the first pseudopodia appeared, which also corresponds to the first occurrence of mucus. This phenomenon is typical of the directed digitated growth, or branching phase, described by numerous authors[27,52–55]. Slime molds developed multiple pseudopodia and did not exhibit any preferential exploration orientation. At the end of the
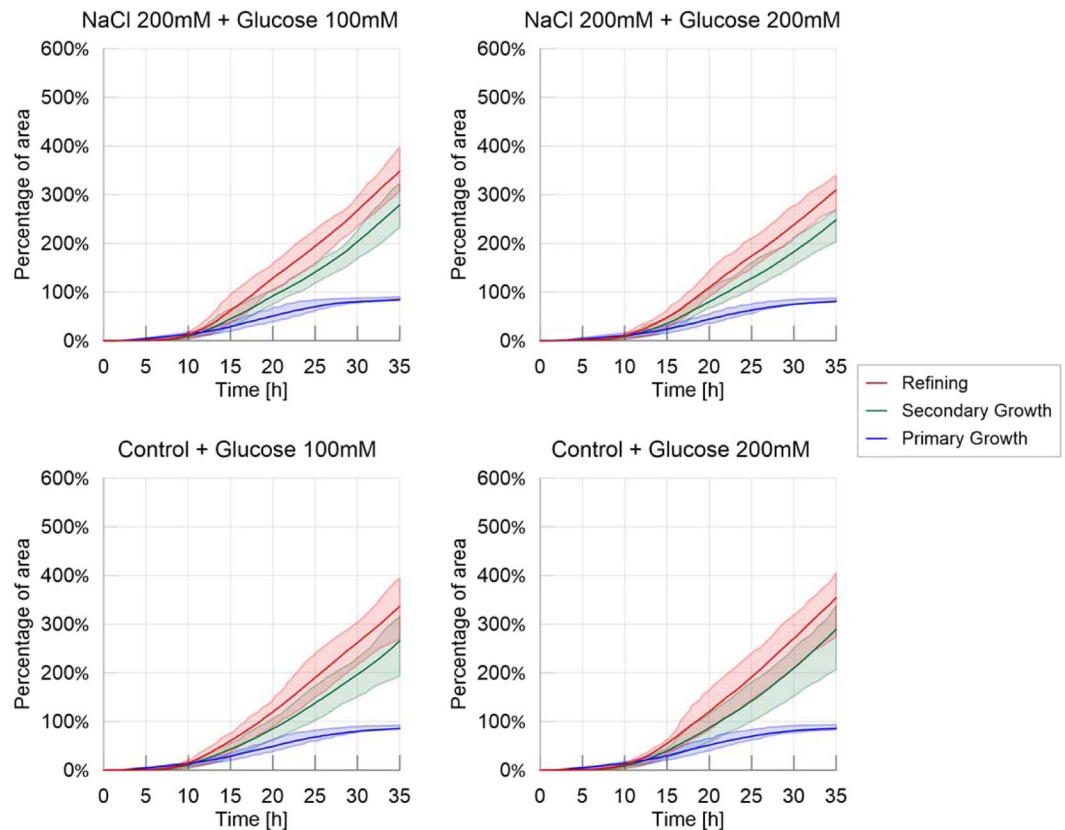
Figure 9. Cumulative areas covered by primary growth, refinement and secondary growth – Spot experiments. The solid line corresponds to the average index calculated over the 20 replicates, while the shaded areas correspond to the first and third quartiles of the data.
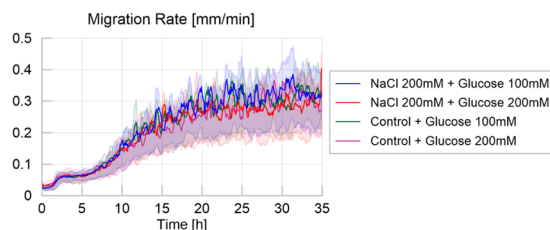

Figure 10. Migration rate over time for the four different treatments, defined as the maximum distance between the contours of the slime mold between two consecutive images, divided by their time interval (5 minutes apart), measured in millimeters per minute. The solid line corresponds to the average calculated over 20 replicates per treatment, while the shaded areas correspond to the first and third quartiles of the data.

experiment, almost all the arena was explored by the slime mold. Thus the exploration was characterized by three phases: (i) Primary growth only, in the quasi-absence of mucus (5–10 hours); (ii) Combination of primary and secondary growth; (iii) Secondary growth only, when the slime mold stops exploring new substrate areas.

Regarding the result obtained for the homogeneous distribution of nutritive cues, we noted first, an environment containing a uniform distribution of nutrients slowed down the exploration of slime mold, mainly by delaying secondary growth and increasing the period of the pulsatile exploration/refinement movements. The area not explored by the slime molds was 3 times larger (respectively 7 times larger) than in the environment deprived of nutrient (control case) for a slightly nutritive (respectively highly nutritive) environment. The exploration rate was almost linear for highly nutritive environments, while for other treatments, the area covered by the slime molds reached a plateau after a period of stretching, which indicates secondary growth and slime mold displacement. This means that slime molds that explored nutritive environments never exhibited a Phase (iii) in their exploration pattern.

Second, on substrates with higher nutrient concentrations, the slime molds grew in a more compact fashion, *i.e.* slime molds presented the highest solidity index and the lowest number of pseudopodia (clusters). Additionally, the appearance of mucus, which indicates that the slime mold was withdrawing, occurred much
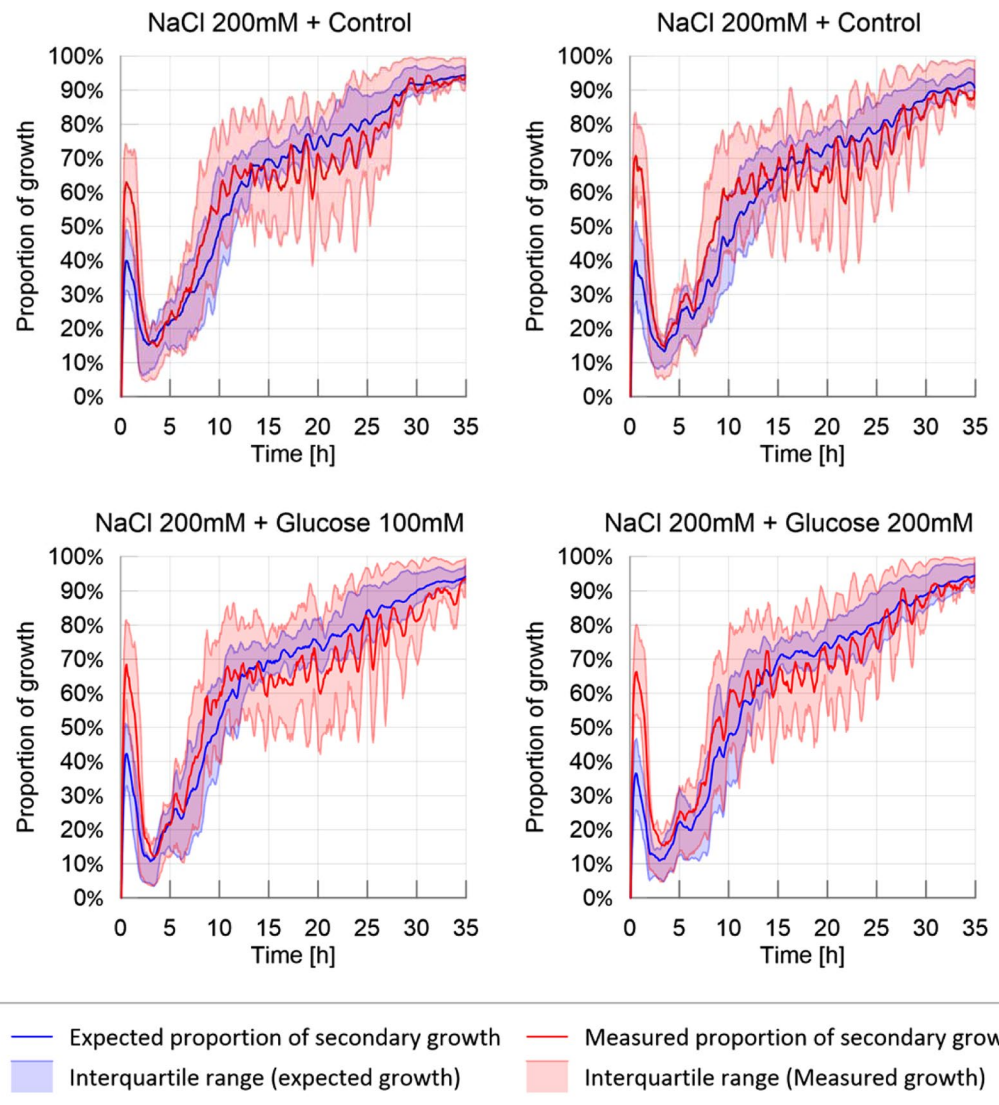
Figure 11. Probability of secondary growth: observed and expected proportion of secondary growth. The solid line corresponds to the average calculated over 20 replicates per treatment, while the shaded areas correspond to the first and third quartiles of the data.

later in nutritive environments. As glucose is only aversive when only above 300 mM[54], our results suggest that nutritive media depressed migration due to feeding behavior. This allows the organism to remain at a site until nutrients are exhausted[56–58]. In previous studies, it was shown that the surface area of substrate covered increases when slime mold responds to nutrient dilution[58,59]. Here, we confirmed these observations and noted that slime mold tended to migrate and grow faster on substrates with the lowest concentration of nutrients, thus maximizing nutrient intake and optimizing the trade-off between nutrient foraging and nutrient intake.

Similarly, for a homogeneous distribution of aversive cues we noted the aversion of slime mold to salt manifested itself through longer contemplative behavior, delayed primary growth and a higher probability to crawl on previously explored surface. In addition, the slime molds grew more compactly and with less pseudopods. This suggests that slime molds were actively avoiding contact with the aversive surface[44,50,60]. In the absence of cell walls, slime mold has no other protection from the environment than mucus. Indeed, in bacteria for instance, mucus is used as protective barrier for the cells against harsh external conditions[61]. In slime molds, the extracellular mucus excreted by the slime molds can have different roles: hydrophilic shield to prevent water loss[62], a lubricating surface over which the slime molds can easily crawl[63], a defensive coat to protect against invasion by foreign materials and organisms[62,64], an aid to phagocytosis[65], a surface that promotes ion-exchange[62] and has externalized spatial memory that helps navigation in unknown environments[26,36,66]. Here, we can add a new function for the mucus i.e. a buffer to move in adverse environment. In other words we demonstrate for the first time that the mucus may be used as a safe haven to avoid prolonged and repeated contacts with hazardous substances encountered in the environment.
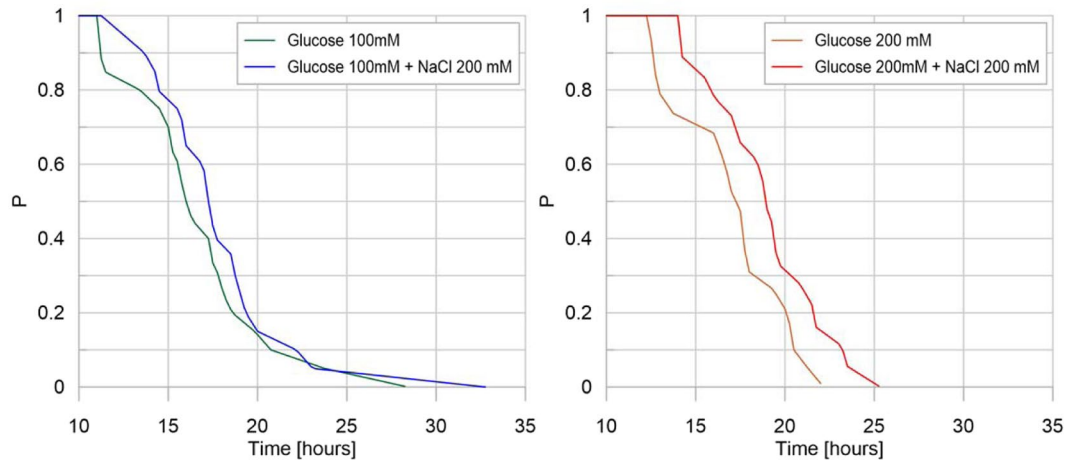
Figure 12. Survival plot: glucose concentration effect. For each treatment, on the vertical axis, the value P corresponds to the fraction of replicates that have not reached the glucose spot at a given time. For a representative number of replicates, P is the probability that glucose has not been reached by slime mold at a given time, for a specific treatment. On the horizontal axis, each value of time corresponds to the average time it takes for a certain fraction of slime mold (P) to reach the glucose spot.

Finally, for non-homogeneous distribution of aversive and non-aversive cues, e.g. spot experiments, pulsatile movements were limited and slime molds responded in the same way regardless of the concentration of glucose used as attractant and regardless of the presence of a salt spot on the way to the glucose spot. Slime molds grew in a more compact fashion, *i.e.* slime molds presented the highest solidity index and the lowest number of pseudopodia (clusters). Additionally, the evolution of the areas covered by slime mold and mucus over time indicates that the response of slime molds to heterogeneous environments was similar to that in the control case. This result suggests that in the spot experiments, the exploration behavior of slime mold is mostly controlled by the substrate. Our observation confirms that salt reception can be affected by the presence of sugars[47]. The authors in[47] showed that the "apparent" enthalpy change accompanying salt perception decreases with increase of sugar concentration.

The proposed image analysis program allows extracting information on expansion rates, geometric changes and probability of occupancy. Ongoing developments aim to acquire high quality images of slime mold exploration tests and to expand the code's capabilities for extracting topological information on the networks formed by slime molds. Slime molds have been shown to be capable of distributed sensing, parallel information processing, and decentralized optimization[39,51,67]. It is also viewed by some researchers as an inspiration for bio-computing devices[68–73]. Our image analysis methods will help such research avenues by improving data collection.

Trajectories of individuals within a flock could also be described to understand whether or not members of the flock can inform and influence the travel direction of other individuals. Such a finding would allow understanding how group decisions are made among gregarious species[74]. The cluster identification and shape recognition program could be used to differentiate modes of gene expression or to recognize objects[75]. Object identification is an important pillar to explain associative memory or to track species interactions in an ecosystem. The tools and approach presented here are thus applicable to any problem of network dynamics or pattern recognition[76].

Methods
Species. *Physarum polycephalum*, also known as the true slime mold, belongs to the Amoebozoa, the sister group to fungi and animals[77]. Slime molds are found on organic substrates where they feed on microorganisms such as bacteria or fungi[77]. The vegetative morph of *P. polycephalum*, the plasmodium, is a vast multinucleate cell that can grow to cover up to a few square meters and crawl at speeds from 0.1 to few centimeters per hour[29,30]. When hygrometry and food availability decrease, the plasmodium turns into an encysted resting stage made of desiccated spherules called sclerotium[29].

Rearing conditions. Experiments were initiated with a total of 10 sclerotia per strain (Southern Biological, Victoria, Australia). We cultivated slime molds on a 1% agar medium with rolled oat flakes, slime molds were fed every day and the medium was replaced daily. Slime molds were 2 weeks old when the experiment started. All experiments were carried out in the dark at 25 °C temperature and 70% humidity, and ran for 35 h. Pictures were taken with a Canon 70D digital camera.

Experimental setup. Initially we monitored the exploration movement evoked in slime molds in a homogeneous environment. Each slime mold was placed in the center of a circular arena (14.5 cm in diameter) with a layer of agar (1% in water) mixed with non-nutritive cellulose (5%). Adding cellulose to the agar mix proved to be useful to obtain a homogeneous pigmentation and to enhance the color contrast between the substrate and slime mold, therefore improving the identification process. A circular hole (2.5 cm in diameter) was punched and
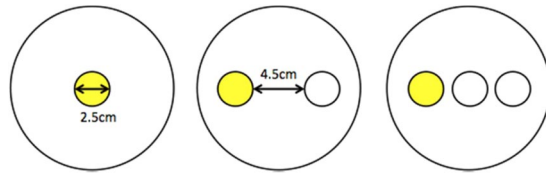
Figure 13. Experimental set-ups for homogenous environment and spot experiment.

replaced with a circular slime mold of the same size sitting on oat. In the first and second treatments (nutritive environments) we added glucose (100 mM or 200 mM) to the medium. In the third treatment (adverse environment), we added a known repellent (NaCl 100 mM[55]) to the medium. Lastly, in the fourth treatment, the medium remained unchanged (neutral environment *i.e.* control treatment).

Subsequently, to investigate how chemotaxis modified the exploration behavior, we introduced discrete spots of attractants/repellents within a neutral substrate made of plain agar. In these so-called "spot experiments", we followed a procedure similar to that for the homogeneous environments. The arena consisted of a 14.5 cm diameter petri dish filled with plain 1% agar mixed with non-nutritive cellulose (5%). Once the agar had set, we punched two or three holes in a line configuration (diameter of each hole 2.5 cm). A circular slime mold (2.5 cm in diameter) was placed diametrically opposite to a glucose (attractant) spot of same size, placed 4.5 cm away. In some of the treatments, a salt (NaCl 200 mM, repellent) spot was added between the slime mold and the attractant spot. A total of 4 different treatments were tested: the first and the second with a single spot of glucose at concentrations of 100 mM and 200 mM respectively, the third and fourth keeping the glucose spots with the same concentrations and adding a NaCl 200 mM spot. Previous experiments show no disruption of slime mold behavior due top punching alone[45].

All slime molds were fed just before the experiment so we assumed that they were in the same physiological state. The experiment consisted of a total of 8 different treatments. We replicated the experiment 20 times for each treatment and monitored each arena for 35 hours taking time-lapse photographs every 5 minutes. Figure 13 shows the experimental set-up for homogeneous environments (left) and discrete distributions of attractants/repellents (right).

Image processing. Time-lapse images were taken every 5 minutes for a total of 420 pictures for each replicate. First, the outside of the petri dish was masked by manually identifying the circular contour; then, the images were converted into the ab* color space (which is the CLAB space without the L* lighting component) since this color space yielded better segmentation results. Then, the clustering algorithm k-means[78,79] was used to classify every pixel into one of two categories or clusters: slime mold or not-slime mold. This last category was further refined based on pixel history, becoming either unexplored surface or mucus. Mucus is the substance left by slime after refinement, which acts as an external memory on explored areas[36,66].

The change of class from unexplored substrate to slime mold, defined as primary growth, means that slime mold reached a point it had never explored. Similarly, secondary growth is the change from mucus to slime mold, meaning that the cell is revisiting a location. Lastly, if the slime mold recedes, e.g. a pixel goes from slime mold to non-slime mold, it becomes mucus, and is defined as refinement. Note that once a pixel is identified as mucus, it can never be classified as unexplored substrate in the following time frames. Two videos are provided as Supplementary Material, S2 and S3 show one replicate as original images and trinarized images respectively.

Image analysis in space and time. We computed indexes to characterize slime mold geometry dynamics and averaged them over the 20 replicates to obtain statistically representative measures. In order to quantify the differences on distinct substrates, we first calculated the fraction of the petri dish area covered by slime mold, mucus and unexplored substrate over time. The total area, the lighting conditions and the test duration were the same for all treatments, both in the homogeneous and spot experiments. Note that glucose only provides energy to slime mold, which is not gaining significant mass during the experiments[58]. In other words, slime mold is changing its area by mostly by stretching and contracting, therefore changing its area density.

We then computed the cumulative area of primary growth, refinement, and secondary growth over the full period of the experiments comparing two consecutive images at the time. The cumulative area covered by primary growth is indicative of the total area of exploration, therefore it is always smaller or equal to the total area of the dish. The cumulative area covered by secondary growth indicates whether slime mold expansion is monotonic (dominated by primary growth) which results in a smaller magnitude, or cyclic (secondary growth dominated, with pulsatile movements) which results in a larger magnitude. The cumulative area covered by refinement indicates slime mold density changes. Within a given time interval, if the area covered by primary plus secondary growth equals that covered by refinement, then slime mold keeps the same density, whereas if it is superior, the slime mold stretches (e.g. density decreases). If secondary growth is negligible and if the area covered by primary growth equals the area covered by refinement, then slime mold displaces mass.

We calculated the extent of growth for each pair of consecutive images as the distance from each pixel where growth occurred (both primary and secondary) to the closest pixel classified as slime mold in the previous image. We calculated the migration rate as the ratio between the maximum extent of growth and the time interval between images (5 min). Then we delineated the region explored by slime mold within the interval as the contour of the slime mold with an offset distance corresponding to the migration rate (see the Supplementary Material Fig. 1 in S1 Appendix for more details).

We estimated the fraction of secondary growth relative to the total number of pixels in the region of expansion. We then calculated the fraction of "expected secondary growth", which would have occurred if secondary growth had happened randomly. If the measured secondary growth fraction is higher (respectively, lower) than the expected one, this means that slime mold has a bias towards mucus (respectively, unexplored substrate).

Additionally, we computed four shape parameters indicative of the contour of slime mold: circularity, eccentricity, solidity and number of clusters. Circularity (C) is defined as:

$$C = P^2/4\pi A$$

where P and A are the perimeter and area of the shape of slime mold at a given time. Eccentricity (E) is calculated as the ratio between the distance between the foci and the major axis length, as follows:

$$E = \sqrt{1 - \left(\frac{b}{a}\right)^2}$$

In which a and b are the lengths of the major and minor axes, respectively. Solidity (S) is the ratio between the area of the slime mold contour and the area of its convex hull. Lastly, we measured the number of clusters by performing an erosion operation along the contour of slime mold, after which only the clusters of high concentration of slime mold remain, which provided the number of pseudopodia or clusters of slime mold.

For the spot experiments, we also determined the distance from the slime mold to the glucose spot at every time, as the minimum distance between the contour of slime mold and the glucose spot. The evolution of the distance to glucose over time was analyzed in a way similar to a survival analysis.

Statistics. The full description of the statistics is provided as part of the Supplementary Information; Appendix S1 includes the statistical procedure and results; while Appendix S4 is an R markdown allowing analysis reproduction. When dependent variables lasted until the occurrence of certain event, we conducted survival analyses using the R package coxme[80]. For the remaining dependent variables, we did linear analyses using the R packages lme4[81] and lmerTest[82]. We tested as fixed factors the four treatments in the homogeneous experiment and both the attracting and the repelling spots and their interaction. The date of the experiment was considered as a random factor. Finally, we performed a nested model comparison using the R package MuMIn[83] by ordering models according to their Akaike criterion and represented the selected model by plotting each estimator, their 95%CI and p-values.

Author summary. *Physarum polycephalum*, also called slime mold, is a giant single-celled organism that can grow to cover several square meters, forming search fronts that are connected to a system of intersecting veins. An original experimental protocol allowed tracking the shape of slime mold placed in homogenous substrates containing an attractant (glucose) or a repellent (salt), or in homogeneous substrates that contained an attractive spot (glucose), an eccentric slime mold and a repulsive spot (salt) in between. For the first time, the rate of exploration of unexplored areas (primary growth) and the rate of extension in previously explored areas (secondary growth) were rigorously measured, by means of a sophisticated image analysis program. This paper shows that the chemical composition of the substrate has more influence on the morphology and growth dynamics of slime mold than that of concentrated spots of chemicals. It was also found that on a repulsive substrate, slime mold exhibits a bias towards secondary growth, which suggests that the mucus produced during slime mold migration acts as a protective shell in adverse environments.

References

1. Ball, P. & Borley, N. R. The self-made tapestry: pattern formation in nature. Vol. 198. Oxford University Press Oxford; (1999).
2. Rietkerk, M. & de Koppel, J. Regular pattern formation in real ecosystems. *Trends Ecol Evol.* **23**(3), 169–75 (2008).
3. Theraulaz, G., Gautrais, J., Camazine, S. & Deneubourg, J.-L. The formation of spatial patterns in social insects: from simple behaviours to complex structures. *Philos Trans R Soc London Ser A Math Phys Eng Sci.* **361**(1807), 1263–82 (2003).
4. Teague, B. P., Guye, P. & Weiss, R. Synthetic morphogenesis. *Cold Spring Harb Perspect Biol.* **8**(9), a023929 (2016).
5. Goodwin, B. C. Unicellular morphogenesis. *Cell Shape Determ Regul Regul Role.* 365–91 (1989).
6. Chalut, K. J. & Paluch, E. K. The actin cortex: a bridge between cell shape and function. *Dev Cell.* **38**(6), 571–3 (2016).
7. Driscoll, M. K. *et al.* Cell shape dynamics: from waves to migration. *PLoS Comput Biol.* **8**(3), e1002392 (2012).
8. Salbreux, G., Charras, G. & Paluch, E. Actin cortex mechanics and cellular morphogenesis. *Trends Cell Biol.* **22**(10), 536–45 (2012).
9. Charras, G. & Sahai, E. Physical influences of the extracellular environment on cell migration. *Nat Rev Mol cell Biol.* **15**(12), 813 (2014).
10. van Helvert, S., Storm, C. & Friedl, P. Mechanoreciprocity in cell migration. *Nat Cell Biol.* **20**(1), 8 (2018).
11. Friedl, P. & Wolf, K. Plasticity of cell migration: a multiscale tuning model. *J Cell Biol.* **188**(1), 11–9 (2010).
12. Gardel, M. L., Schneider, I. C., Aratyn-Schaus, Y. & Waterman, C. M. Mechanical integration of actin and adhesion dynamics in cell migration. *Annu Rev Cell Dev Biol.* **26**, 315–33 (2010).
13. Inagaki, N. & Katsuno, H. Actin waves: Origin of cell polarization and migration? *Trends Cell Biol.* **27**(7), 515–26 (2017).
14. Aman, A. & Piotrowski, T. Cell migration during morphogenesis. *Dev Biol.* **341**(1), 20–33 (2010).
15. Reig, G., Pulgar, E. & Concha, M. L. Cell migration: from tissue culture to embryos. *Development.* **141**(10), 1999–2013 (2014).
16. Yamada, K. M. & Mayor, R. Cell dynamics in development, tissue remodelling, and cancer. *Curr Opin Cell Biol.* **42**, iv (2016).
17. Hind, L. E., Vincent, W. J. B. & Huttenlocher, A. Leading from the back: the role of the uropod in neutrophil polarization and migration. *Dev Cell.* **38**(2), 161–9 (2016).
18. Mseka, T., Bamburg, J. R. & Cramer, L. P. ADF/cofilin family proteins control formation of oriented actin-filament bundles in the cell body to trigger fibroblast polarization. *J Cell Sci.* **120**(24), 4332–44 (2007).
19. King, J. S. & Insall, R. H. Chemotaxis: finding the way forward with Dictyostelium. *Trends Cell Biol.* **19**(10), 523–30 (2009).
20. Iglesias, P. A. & Devreotes, P. N. Navigating through models of chemotaxis. *Curr Opin Cell Biol.* **20**(1), 35–40 (2008).

21. Larsen, S. H., Adler, J., Gargus, J. J. & Hogg, R. W. Chemomechanical coupling without ATP: the source of energy for motility and chemotaxis in bacteria. *Proc Natl Acad Sci.* **71**(4), 1239–43 (1974).
22. Nakaoka, Y. & Iwatsuki, K. Hyperpolarization-activated inward current associated with the frequency increase in ciliary beating of Paramecium. *J Comp Physiol A.* **170**(6), 723–7 (1992).
23. Saranak, J. & Foster, K. W. Rhodopsin guides fungal phototaxis. *Nature.* **387**(6632), 465 (1997).
24. Nakagaki, T., Yamada, H. & Tóth, A. Maze-solving by an amoeboid organism. *Nature [Internet].* **407**(6803), 470, Available from, http://www.ncbi.nlm.nih.gov/pubmed/11028990 (2000).
25. Kuroda, S., Takagi, S., Nakagaki, T. & Ueda, T. Allometry in Physarum plasmodium during free locomotion: size versus shape, speed and rhythm. *J Exp Biol.* **218**(23), 3729–38 (2015).
26. Rodiek, B. & Hauser, M. J. B. Migratory behaviour of Physarum polycephalum microplasmodia. *Eur Phys J Spec Top.* **224**(7), 1199–214 (2015).
27. Vogel, D. *et al.* Phenotypic variability in unicellular organisms: from calcium signalling to social behaviour. *Proc R Soc B Biol Sci.* **282**(1819), 20152322 (2015).
28. Vogel, D., Dussutour, A. & Deneubourg, J.-L. Symmetry breaking and inter-clonal behavioural variability in a slime mould. *Biol Lett.* **14**(12), 20180504 (2018).
29. Aldrich, H. Cell biology of Physarum and Didymium V1: organisms, nucleus, and cell cycle. Elsevier (2012).
30. Oettmeier, C., Brix, K. & Döbereiner, H.-G. Physarum polycephalum—A new take on a classic model system. *J Phys D Appl Phys.* **50**(41), 413001 (2017).
31. Ueda, T. Pattern dynamics in cellular perception. *Phase Transitions A Multinatl J.* **45**(2–3), 93–104 (1993).
32. Kuroda, R. & Kuroda, H. Relation of cytoplasmic calcium to contractility in Physarum polycephalum. *J Cell Sci.* **53**(1), 37–48 (1982).
33. Yoshimoto, Y., Matsumura, F. & Kamiya, N. Simultaneous oscillations of Ca2+ efflux and tension generation in the permealized plasmodial strand of Physarum. *Cell Motil.* **1**(4), 433–43 (1981).
34. Farr, D. R., Amster, H. & Horisberger, M. Composition and partial structure of the extracellular polysaccharide of Physarum polycephalum. *Carbohydr Res.* **24**(1), 207–9 (1972).
35. Sesaki, H. & Ogihara, S. Secretion of slime, the extracellular matrix of the plasmodium, as visualized with a fluorescent probe and its correlation with locomotion on the substratum. *Cell Struct Funct.* **22**(2), 279–89 (1997).
36. Reid, C. R., Latty, T., Dussutour, A. & Beekman, M. Slime mold uses an externalized spatial "memory" to navigate in complex environments. *Proc Natl Acad Sci.* **109**(43), 17490–4 (2012).
37. Reid, C. R. & Beekman, M. Solving the Towers of Hanoi - how an amoeboid organism efficiently constructs transport networks. *J Exp Biol [Internet].* **216**, 1546–51, Available from, http://www.ncbi.nlm.nih.gov/pubmed/23307798 (2013).
38. Ueda, T., Hirose, T. & Kobatake, Y. Membrane biophysicsdf chemoreception and taxis in the plasmodium of physarum polycephalum. *Biophys Chem.* **11**(3–4), 461–73 (1980).
39. Reid, C. R. & Latty, T. Collective behaviour and swarm intelligence in slime moulds. *FEMS Microbiol Rev.* **40**(6), 798–806 (2016).
40. Saigusa, T., Tero, A., Nakagaki, T. & Kuramoto, Y. Amoebae anticipate periodic events. *Phys Rev Lett.* **100**(1), 18101 (2008).
41. Tero, A. *et al.* Rules for biologically inspired adaptive network design. *Science [Internet].* 2010 Jan 22, **327**(5964), 439–42, Available from, http://www.ncbi.nlm.nih.gov/pubmed/20093467 [cited 2018 Nov 21].
42. Latty, T. *et al.* Slime moulds use heuristics based on within-patch experience to decide when to leave. *J Exp Biol [Internet].* **218**(Pt 8), 1175–9, Available from, http://www.ncbi.nlm.nih.gov/pubmed/25722006 (2015).
43. Reid, C. R., Garnier, S., Beekman, M. & Latty, T. Information integration and multiattribute decision making in non-neuronal organisms. *Anim Behav.* **100**, 44–50 (2015).
44. Boisseau, R. P., Vogel, D. & Dussutour, A. Habituation in non-neural organisms: evidence from slime moulds. *Proc R Soc B Biol Sci.* **283**(1829), 20160446 (2016).
45. Dussutour, A., Ma, Q. & Sumpter, D. Phenotypic variability predicts decision accuracy in unicellular organisms. *Proc R Soc B.* **286**(1896), 20182825 (2019).
46. Adamatzky, A. Slime Mold Solves Maze in One Pass, Assisted by Gradient of Chemo-Attractants. *IEEE Trans Nanobioscience [Internet].* 2012 Jun, **11**(2), 131–4, Available from, http://ieeexplore.ieee.org/document/6148283/ [cited 2019 Aug 8].
47. Terayama, K., Ueda, T., Kurihara, K. & Kobatake, Y. Effect of sugars on salt reception in true slime moldPhysarum polycephalum. *J Membr Biol.* **34**(1), 369–81 (1977).
48. Carlile, M. J. Nutrition and chemotaxis in the myxomycete Physarum polycephalum: the effect of carbohydrates on the plasmodium. *Microbiology.* **63**(2), 221–6 (1970).
49. Ueda, T., Terayama, K., Kurihara, K. & Kobatake, Y. Threshold phenomena in chemoreception and taxis in slime mold Physarum polycephalum. *J Gen Physiol.* **65**(2), 223–34 (1975).
50. Ueda, K., Takagi, S., Nishiura, Y. & Nakagaki, T. Mathematical model for contemplative amoeboid locomotion. *Phys Rev E.* **83**(2), 21916 (2011).
51. Jones, J. Characteristics of Pattern Formation and Evolution in Approximations of Physarum Transport Networks. *Artif Life [Internet].* 2010 Apr. **16**(2), 127–53. Available from, http://www.ncbi.nlm.nih.gov/pubmed/20067403 [cited 2019 Aug 8].
52. Halvorsrud, R. & Wagner, G. Growth patterns of the slime mold Physarum on a nonuniform substrate. *Phys Rev E.* **57**(1), 941 (1998).
53. Nakagaki, T., Yamada, H. & Ueda, T. Interaction between cell shape and contraction pattern in the Physarum plasmodium. *Biophys Chem.* **84**(3), 195–204 (2000).
54. Latty, T. & Beekman, M. Food quality affects search strategy in the acellular slime mould, Physarum polycephalum. *Behav Ecol.* **20**(6), 1160–7 (2009).
55. Vogel, D. & Dussutour, A. Direct transfer of learned behaviour via cell fusion in non-neural organisms. *Proc R Soc B Biol Sci.* **283**(1845), 20162382 (2016).
56. Knowles, D. J. C. & Carlile, M. J. The chemotactic response of plasmodia of the myxomycete Physarum polycephalum to sugars and related compounds. *Microbiology.* **108**(1), 17–25 (1978).
57. Daniel, J. W. & Baldwin, H. H. Methods of culture for plasmodial myxomycetes. In: Methods in Cell Biology. Elsevier; 1964. p. 9–41.
58. Dussutour, A., Latty, T., Beekman, M. & Simpson, S. J. Amoeboid organism solves complex nutritional challenges. *Proc Natl Acad Sci.* **107**(10), 4607–11 (2010).
59. Takamatsu, A., Takaba, E. & Takizawa, G. Environment-dependent morphology in plasmodium of true slime mold Physarum polycephalum and a network growth model. *J Theor Biol.* **256**(1), 29–44 (2009).
60. Adamatzky, A. Routing Physarum with repellents. *Eur Phys J E [Internet].* 2010 Apr 17 [cited 2019 Aug 8] **31**(4), 403–10. Available from, https://doi.org/10.1140/epje/i2010-10589-y.
61. Nwodo, U., Green, E. & Okoh, A. Bacterial exopolysaccharides: functionality and prospects. *Int J Mol Sci.* **13**(11), 14002–15 (2012).
62. McCormick, J. J., Blomquist, J. C. & Rusch, H. P. Isolation and characterization of a galactosamine wall from spores and spherules of Physarum polycephalum. *J Bacteriol.* **104**(3), 1119–25 (1970).
63. Simon, H. L. & Henney, H. R. Chemical composition of slime from three species of myxomycetes. *FEBS Lett.* **7**(1), 80–2 (1970).
64. Asgari, M. & Henney, J. H. R. Inhibition of growth and cell wall morphogenesis of Bacillus subtilis by extracellular slime produced by Physarum flavicomum. *Cytobios.* **20**(79–80), 163–77 (1977).
65. Haskins, E. F. & Hinchee, A. A. Light-and ultra-microscopical observations on the surface structure of the protoplasmodium, aphanoplasmodium, and phaneroplasmodium (Myxomycètes). *Can J Bot.* **52**(8), 1835–9 (1974).

66. Reid, C. R., Beekman, M., Latty, T. & Dussutour, A. Amoeboid organism uses extracellular secretions to make smart foraging decisions. *Behav Ecol.* **24**(4), 812–8 (2013).
67. Adamatzky, A. Physarum Machines [Internet]. WORLD SCIENTIFIC; 2010 [cited 2019 Aug 8]. (World Scientific Series on Nonlinear Science Series A; vol. 74). Available from, https://doi.org/10.1142/7968.
68. Adamatzky, A. Advances in physarum machines: sensing and computing with slime mould. 1st edition 2016. Springer International Publishing: Imprint: Springer, 2016. 839 p. (Emergence, Complexity and Computation).
69. Schumann, A. & Adamatzky, A. PHYSARUM SPATIAL LOGIC. *New Math Nat Comput [Internet].* 2011 Sep 21 [cited 2019 Aug 8], **07**(03), 483–98. Available from, https://doi.org/10.1142/S1793005711002037.
70. Adamatzky, A. Physarum machines: encapsulating reaction–diffusion to compute spanning tree. *Naturwissenschaften [Internet].* 2007 Nov 14 [cited 2019 Aug 8] 94(12), 975–80. Available from, http://www.ncbi.nlm.nih.gov/pubmed/17603779.
71. Adamatzky, A. & Jones, J. Towards Physarum Robots: Computing and Manipulating on Water Surface. *J Bionic Eng [Internet].* 2008 Dec 1 [cited 2019 Aug 8] 5(4), 348–57. Available from, https://www.sciencedirect.com/science/article/pii/S1672652908601808.
72. Adamatzky, A., Martínez, G. J., Chapa-Vergara, S. V., Asomoza-Palacio, R. & Stephens, C. R. Approximating Mexican highways with slime mould. *Nat Comput [Internet].* 2011 Sep 28 [cited 2019 Aug 8] 10(3), 1195–214. Available from, https://doi.org/10.1007/s11047-011-9255-z.
73. Umedachi, T., Takeda, K., Nakagaki, T., Kobayashi, R. & Ishiguro, A. Fully decentralized control of a soft-bodied robot inspired by true slime mold. *Biol Cybern [Internet].* 2010 Mar 4 [cited 2019 Aug 8] 102(3), 261–9. Available from, https://doi.org/10.1007/s00422-010-0367-9.
74. Couzin, I. D. Collective cognition in animal groups. *Trends Cogn Sci.* **13**(1), 36–43 (2009).
75. Olshausen, B. A., Anderson, C. H. & Van Essen, D. C. A neurobiological model of visual attention and invariant pattern recognition based on dynamic routing of information. *J Neurosci.* **13**(11), 4700–19 (1993).
76. Tamayo, P. *et al.* Interpreting patterns of gene expression with self-organizing maps: methods and application to hematopoietic differentiation. *Proc Natl Acad Sci.* **96**(6), 2907–12 (1999).
77. Stephenson, S. L. & Schnittler, M. Myxomycetes. *Handb Protists.* 1405–31 (2017).
78. Kanungo, T. *et al.* An efficient k-means clustering algorithm: Analysis and implementation. *IEEE Trans Pattern Anal Mach Intell.* **7**, 881–92 (2002).
79. Dhanachandra, N., Manglem, K. & Chanu, Y. J. Image Segmentation Using K -means Clustering Algorithm and Subtractive Clustering Algorithm. *Procedia Comput Sci [Internet].* 2015 Jan 1 [cited 2019 Aug 8] 54, 764–71. Available from, https://www.sciencedirect.com/science/article/pii/S1877050915014143.
80. Therneau, T. A Package for Survival Analysis in S. version 2.38. (2015).
81. Bates, D., Sarkar, D., Bates, M. D. & Matrix, L. The lme4 package. *R Packag version.* **2**(1), 74 (2007).
82. Kuznetsova, A., Brockhoff, P. B. & Christensen, R. H. B. lmerTest package: tests in linear mixed effects models. *J Stat Softw.* **82**, 13 (2017).
83. Barton, K. & Barton, M. K. Package 'MuMIn' Version 1. 2015.

Acknowledgements

Author contributions

Author Fernando Patino-Ramirez (F.P.) carried out the image analysis, wrote the corresponding sections about methods and results created the figures in the manuscript and was responsible of the image analysis section on S1 and the videos S2 and S3. A.B. developed the statistical analysis, including the corresponding sections in Supplementary Materials S1 and S4. Authors Aurèle Boussard (A.B.) and Audrey Dussutour (A.D.) carried out the experiments in the laboratory and the corresponding image acquisition. Chloé Arson (C.A.) drafted the manuscript and contributed in the planning, analysis and interpretation of the experiments and the data together with A.D., F.P. and A.B. All the authors have approved the submitted version of this manuscript and have agreed both to be accountable for the author's own contributions.

Competing interests

The authors declare no competing interests.

Additional information

Supplementary information is available for this paper at https://doi.org/10.1038/s41598-019-50872-z.

Correspondence and requests for materials should be addressed to F.P. or A.D.

Reprints and permissions information is available at www.nature.com/reprints.

Publisher's note Springer Nature remains neutral with regard to jurisdictional claims in published maps and institutional affiliations.